1-1-2019

Stabilization of DNA i-motif structures by 7-aminoactinomycin D, an anti-tumor drug

Justin Lane Parmely

STABILIZATION OF I-MOTIF DNA STRUCTURES BY 7-AMINOACTINOMYCIN D, AN ANTI-TUMOR DRUG

A Thesis
presented in partial fulfillment of requirements
for the degree of Master of Science
in the Department of Chemistry & Biochemistry
The University of Mississippi

By

JUSTIN LANE PARMELY

AUGUST 2019

ABSTRACT

Alternative DNA structures are likely to form from Watson-Crick B-form DNA when there is an asymmetric distribution of guanosine and cytosine on opposite DNA strands, especially during processes that involve superhelical duress. A guanosine rich strand can form a four-stranded structure known as a G-quadruplex (G4). The complimentary cytosine rich strand can utilize intercalating cytosine-cytosine base pairing to form a four-stranded structure known as an i-motif (iM). While both structures are known to exist *in vivo*, they are energetically uphill from double strand DNA (dsDNA), meaning that additional factors are needed to facilitate their formation. Earlier, it was believed that iMs required slightly acidic conditions (pH $\leq$ 6) for structure stabilization. However, crowding agents like polyethylene glycols and dextrans can shift the pKa of the iM (the pH at which 50% of the iM is folded) nearer to the physiological pH of ~7. Additionally, loop regions of iMs have been implicated in their thermal and pH-dependent stability. Small molecules such as polyamines and larger molecules like proteins can interact with iMs by binding to their loops, suggesting that additional biochemical factors may also facilitate their stabilization. In this report, we present data on how 7-aminoactinomycin D -- an antitumor drug known to bind DNA loops -- can affect the iM structure. Our results demonstrate that a small molecule antitumor drug can stabilize or destabilize iMs by simultaneously changing thermodynamic properties including Tm, pKa, and $\Delta G^{\circ}_{37\ ^{\circ}C}$. Our results suggest that the use of small molecules may be a promising way to therapeutically regulate expression of genes controlled by alternative DNA structures like G4s and iMs.

LIST OF ABBREVIATIONS AND SYMBOLS

dsDNA	double-stranded DNA
ssDNA	single-stranded DNA
7-AAMD	7-Aminoactinomycin D
AMD	Actinomycin D
iM	i-Motif
G4	G-Quadruplex
T_m	Melting Temperature
K_d	Dissociation Constant
CD	Circular Dichroism

ACKNOWLEDGEMENTS

I would like to thank the National Science Foundation (CHE-1156713) for originally funding my position as an undergraduate summer research student. I would also like to thank the National Institute of Health (1P50CA13080501A1) for allowing me to continue that work.

I would like to personally thank my advisor, Dr. Randy Wadkins, whose previous work laid the foundation for this project; without his guidance, this project could not have been completed.

I would like to thank Dr. Saumen Chakraborty and Dr. James Cizdziel as members of my thesis committee for providing valuable feedback on my project and manuscript.

Additionally, I would like to thank Dr. Tracy Brooks, who first showed me what it meant to be an impassioned researcher.

Lastly, I would like to extend a special thanks to Harrison Davis, Adam Weekley, and Sarai Jaime, undergraduates who have played important roles throughout the duration of this project.

TABLE OF CONTENTS

LIST OF FIGURES

CHAPTER I: INTRODUCTION

The DNA inside eukaryotic nuclei exists predominantly in the familiar double helix B-form conformation, as first reported by Watson and Crick.[1] However, there are many instances when this familiar conformation can be altered. Intranuclear processes like transcription and replication locally unwind and melt dsDNA into two single strands of DNA (ssDNA), which in turn allows for the formation of non B-form DNA structures.[2] Non-B DNA structures—sometimes referred to as DNA secondary structures—are thought to play several different roles in cells, including regulation of transcription.[3,4] Interestingly, regions of ssDNA rich in guanosine and cytosine have shown the ability to form noncanonical, four-stranded DNA structures called G-quadruplexes (G4) and i-Motifs (iM), respectively.

The G4 structure is made possible through Hoogsteen hydrogen bonding between four guanosine residues on a single strand of DNA. These residues interact with one another to form a planar tetrad; in regions of ssDNA rich in guanosine, multiple tetrads can form and stack on one another, forming the G4.[5] Multiple factors contribute to the formation and stability of these structures, including solvent-makeup, monovalent cations, protein binding, and superhelical duress.[6-8] G4s are known to form *in vivo*,[5] and the sequences of DNA capable of forming G4s are disproportionately located in and around the promoter elements of proto-oncogenes; there has been much work over the years describing the variations in the likely mechanisms by which different G4s affect transcription of genes,[9] but the overall results suggest G4s represent a potential drug target to therapeutically manipulate expression of oncogenes.

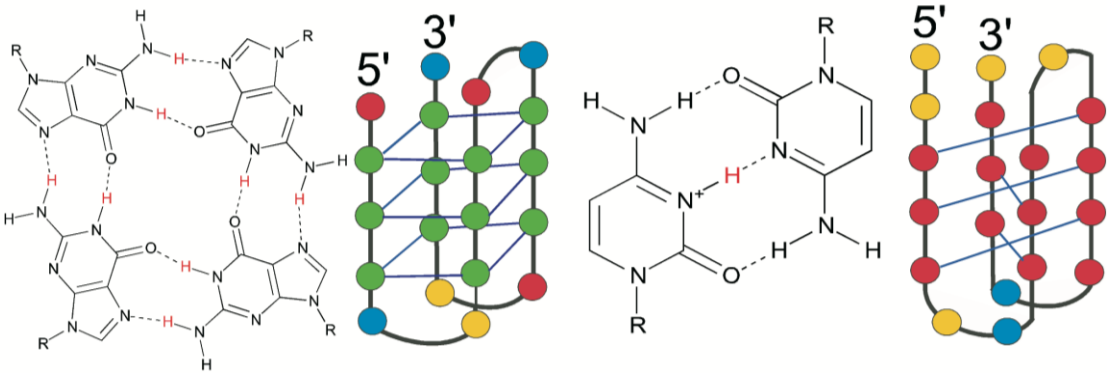

Figure 1. Schematic describing the general structure of G4s and iMs formed from ssDNA. Guanosine residues are shown in green, and cytosine residues are shown in red.

The cytosine rich DNA complementary to guanosine rich sequences are similarly capable of forming a ssDNA structure called the iM. Their existence was first proposed in the 1960's when Landridge and Rich[10] postulated that DNA containing multiple protonated cytosines could hydrogen bond with one another at low pH to form an ordered structure. The existence of such structures was not validated until the 1990's.[11] At pH near 5.4, a poly-dC strand of DNA becomes partially ionized, allowing for noncanonical, hemiprotonated C•C^+ base pairs to intercalate with one another and form the iM.[11] However, early studies of iM stability revealed that the proton concentrations necessary to form the C•C^+ base pairs are only readily available at relatively acidic pH's (below pH 6), which is significantly more acidic than the intranuclear pH of ~7.1. As a result, the iM was initially regarded as a biophysical novelty with no real physiological relevance.

The early experiments on iMs, however, did not consider the different biochemical factors that could influence formation of iMs *in vivo*. For example, experiments have shown that the activity of water can affect the formation of ssDNA structures like the iM.[12,13] Approximately 20%-40% of the volume of eukaryotic cell nuclei is occupied not by water, but by biomolecules.[14] In this crowded intranuclear environment, water activity is measurably lower than in the dilute aqueous buffer first used to understand the pH-dependent formation of iMs. The use of crowding

agents such as polyethylene glycols and dextrans to mimic the crowded nuclear environment reveals an almost universal shift in the stability of iMs toward more physiologically relevant values.[12,15-17] These studies suggest that iM structures are more stable at physiological pH than originally anticipated.

Recently, iM structures have been directly observed in cell nuclei, confirming that their formation from dsDNA *in vivo* is energetically possible, thus further increasing interest in their possible biological role. Some of the most exciting work has come from the labs of Dinger and Christ, who have recently published the first visualization of native iMs in the nuclei of human cell lines.[18] The formation of iM structures was not only pH-dependent -- as expected -- but also cell-cycle dependent; iM formation was most prevalent at the G1/S boundary, a point in the cell-cycle where transcriptional activity is high, providing further evidence that iMs, like G4s, serve an important role in transcriptional regulation.

Because iM-forming sequences of DNA are complementary to G4-forming sequences of DNA, the sequences that are capable of forming iMs are also predominantly located in and around promoter elements of proto-oncogenes, and investigations into the iM as a transcriptional regulator have been fruitful.[9,19-25] For example, the Hurley lab has proposed a mechanism by which an iM in the promoter of the *myc* gene affects transcription of the gene by acting as a mechanosensor.[26] In cases of minimal negative supercoiling in the *myc* promoter, iM folding is facilitated, and the binding of important transcription factors to this cytosine-rich region is inhibited, leading to lowered transcription of the *myc* gene. When the same promoter becomes more densely supercoiled, iM folding is inhibited and the unfolded ssDNA conformation is more favored. The unfolded iM facilitates binding of transcription factors, and transcription of *myc* increases. This is a very important finding, as it appears to confirm what has long been expected about the role of

G4s and iMs in gene regulation.

Attempts to understand the biological roles of iMs as transcriptional regulators -- and ultimately, as drug targets -- have required the identification of iM-interactive compounds. Of the few compounds known to interact with iMs, many are inspired by preexisting compounds that interact with G4s. Examples include Tetra-(*N*-methyl-4-pyridyl) porphyrin;[27] macrocyclic poly-oxazoles;[28] and several phenanthroline and acridine derivatives.[29,30] Screening chemical databases has identified other iM-interactive compounds such as mitoxantrone, a synthetic doxorubicin derivative; tilorone, an antiviral compound; and tobramycin, an aminoglycoside antibiotic.[31]

The identification of iM-interactive compounds has allowed researchers to understand iM function associated with other proto-oncogenes like *bcl-2*.[32,33] Upstream of the *bcl-2* gene's P1 promoter is a GC-rich element integral to *bcl-2* promoter activity; deletions or mutations in this region lead to elevated transcription of *bcl-2*. The cytosines within this element are capable of forming an iM.[23] Hurley et al., identified two compounds -- IMC-76, a cholestane derivative, and IMC-48, a pregnanol derivative -- that have opposing effects on the stability of this *bcl-2* iM *ex vivo*. IMC-76 was shown to unfold the iM into a hairpin conformation, and IMC-48 was shown to stabilize the folded version of the iM. Treating *bcl-2* positive cancer cell lines with these compounds resulted in opposite effects on transcription of the *bcl-2* gene. Use of IMC-76 lead to a downregulation in transcription of *bcl-2*, resensitizing lymphoma cell lines to treatment with traditional chemotherapy. In xenograft murine lymphoma models, use of IMC-76 alongside a *myc* G4-interactive compound substantially lowered the IC_{50} values of traditional chemotherapy agents.[34] These papers give further evidence that iMs affect transcription via their folded or unfolded state, and furthermore, that the distribution of these conformations can be affected by the use of small molecules.

Other iM-interactive compounds have been used to probe the function of iMs associated with other proto-oncogenes.[35] The Hurley lab has shown that expression of the oncogene *KRAS* can be regulated with an iM-interactive benzophenanthridine alkaloid.[36] Additionally, they have described an iM-interactive benzothiophene-2-carboxamide with the ability to affect transcription of *PDGFR-β* in neuroblastoma cell lines.[37] Shu et al., have recently synthesized an acridone derivative that has the ability to selectively bind and stabilize the *myc* promoter iM; their *in vitro* data shows this compound can downregulate the oncogenic overexpression of *myc*.[38] While the iMs associated with each of these proto-oncogenes regulates transcription differently, a pattern has emerged: small molecules that affect the equilibrium of the folded and unfolded iM can impact transcription of genes controlled by iMs.

Ligands like those mentioned above have helped researchers to understand some of the biological roles that iMs play, but their usefulness in the study of other iMs is limited because the ability of these compounds to target iMs is heavily dependent on the structural features of the iM. This is important to note, because iMs constitute a diverse class of DNA structures that can vary in cytosine tract length, loop length, loop position, and loop composition. To understand the feasibility of the iM as a drug target, future studies of iMs will necessitate new iM-interactive compounds, but the identification of novel iM-interactive compounds is a difficult process with very low success rates. Conventional drug discovery methods will likely be slow to identify iM-interactive compounds, impeding our ability to draw broader conclusions about small molecule targeting of the iM.

The structural diversity of iMs, however, also grants us the freedom to create unique models to study the effects of ligand binding to the iM. In this thesis, a series of non-genomic "model" iMs (**Fig. 4**) were synthesized that facilitate interaction with a known DNA binding drug,

7-Aminoactinomycin D, to assess the ability of a small molecule to affect the overall stability of the iM. We found that a small, loop-binding molecule like 7-AAMD can modestly affect overall iM stability. However, these changes were less dramatic than anticipated, suggesting that small loop-binding molecules may not be the best method to dramatically affect iM stability.

CHAPTER II: BINDING OF 7-AAMD TO MODEL IMS

II.a Introduction

The iM forms of DNA have been implicated as important transcriptional regulators of genes, predominantly those that are often misregulated in cancer. As such, they are appealing drug targets. The use of small molecules to affect the stability of these iMs seems a promising way to affect gene expression, with potential anti-cancer benefits.[32-34] but due to difficulty identifying iM-interactive compounds, little is known about the extent to which small molecules can affect the stability of iMs. By creating seven, non-genomic model iMs (**Fig. 4**) that facilitated strong interaction with 7-aminoactinomycin D (7-AAMD), a known DNA-binding fluorophore derived from actinomycin D (AMD), the ability of small molecules to affect iM stability was studied.

7-AAMD is the fluorescent analogue of AMD, a potent antiviral and anticancer molecule isolated from bacteria of the genus *Streptomyces*. The molecule (**Fig. 2**) is composed of a planar phenoxazone chromophore linked to two identical, pentapeptide rings. 7-AAMD's therapeutic properties were once broadly attributed to the molecule's ability to nonspecifically bind guanosine residues via intercalation, halting transcription by RNA polymerase,[39-43] but later studies of 7-AAMD revealed the molecule's unique and much higher affinity for ssDNA target sequences

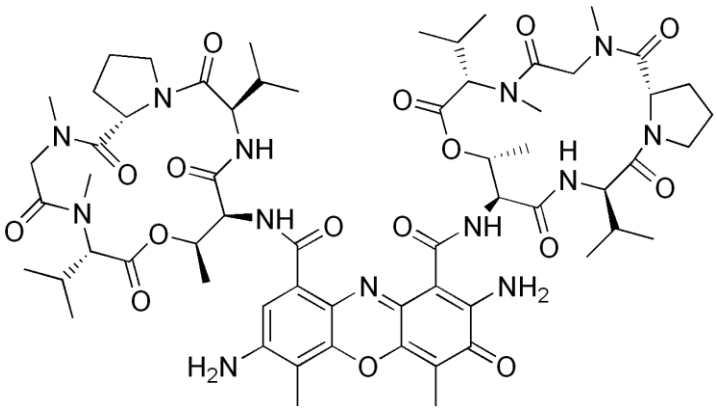

Figure 2. The structure of 7-AAMD. For simplicity, the identical pentapeptide rings are shown coplanar with the phenoxazone; in reality, they are above and below the plane of the paper.

that contain 5'-AGT-3', especially when those sequences can form a ssDNA hairpin.[44-47] This hairpin ssDNA secondary structure can recruit AMD, and via "hemi-intercalation" of the phenoxazone into the 5'-AG-3' polypurine step and coordination of the pentapeptide rings with nearby bases in the loop of the DNA hairpin, the drug can stabilize the secondary structure.[46] The ability of 7-AAMD to bind and stabilize a ssDNA target will be fundamental to our studies.

7-AAMD's affinity for this target was discovered by pronounced changes to the molecule's emission spectra upon binding to ssDNA, changes that are useful for studies of drug-DNA interactions. Upon binding the target hairpin DNA, 7-AAMD's fluorescence intensifies dramatically and undergoes a pronounced hypsochromic shift.[44] Understanding the unique environment in which 7-AAMD resides when bound to these ssDNA hairpins helps to explain the observed changes in the emission spectra. 7-AAMD "identifies" its target by simultaneous intercalation between purine base pairs in the stem-loop interface and hydrogen bonding of a pentapeptide ring with nearby DNA bases in the loop of the hairpin. Interestingly, in the hairpins studied, non-Watson-Crick mismatched base pairs like T-T in the stem of the DNA hairpin help to stabilize the DNA-drug complex while simultaneously shielding the fluorophore from water. Without nearby water, the excited state of 7-AAMD does not experience as much hydrogen bonding with the surrounding solvent. As a result, energy is less effectively dissipated in 7-AAMD's excited state, and this energy is instead released via emission, resulting in a blue shift of the emission spectrum.[48] The hydrophobic environment of the bound 7-

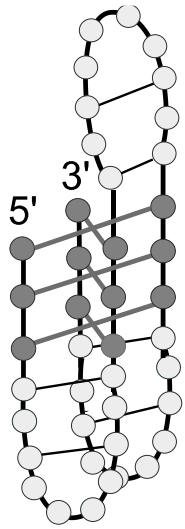

Figure 3. The folded model iM L123HP with labeled loop regions. Each of the seven model iMs contains the hairpin loop known to bind 7-AAMD; the name of each model iM describes the placement of the loop.

AAMD also liberates the fluorophore from solvent-mediated quenching, and as a result, more intense fluorescence can be detected; quantum yield efficiencies can grow more than five-fold if the "hydrophobic matching" of 7-AAMD to the ssDNA structure is ideal.[44-46,48] These unique changes in the emission spectrum of 7-AAMD position the drug as a great tool for studying interactions with ssDNA structures like the iM.

Model iM Sequences

L1HP	5'-CCC**AGTTTTAAA**TCCCTCCCTCCC-3'
L2HP	5'-CCCTCCC**AGTTTTAAA**TCCCTCCC-3'
L3HP	5'-CCCTCCCTCCC**AGTTTTAAA**TCCC-3'
L12HP	5'-CCC**AGTTTTAAA**TCCC**AGTTTTAAA**TCCCTCCC-3'
L13HP	5'-CCC**AGTTTTAAA**TCCCTCCC**AGTTTTAAA**TCCC-3'
L23HP	5'-CCCTCCC**AGTTTTAAA**TCCC**AGTTTTAAA**TCCC-3'
L123HP	5'-CCC**AGTTTTAAA**TCCC**AGTTTTAAA**TCCC**AGTTTTAAA**TCCC-3'

Figure 4. The seven model ssDNA iMs used in these studies. The hairpin loops (shown in bold) are a known target of 7-AAMD. The name of each model iM describes the loop position of the hairpin sequence.

AIM OF THESIS: The specific aim of this thesis is to assess the stability of seven model iMs before and after binding of a known anti-tumor drug, 7-AAMD. 7-AAMD is known to have a strong affinity for a ssDNA hairpin.[46] The seven model iMs incorporate this hairpin target into their loop regions; these loop regions are diverse structural features of iMs that play important roles in biomolecular recognition of genomic iMs.[33,49] Given the high affinity of 7-AAMD for the hairpin loops, we can begin to understand the extent to which small molecules can affect iM stability when they interact with this important iM structural feature. This is important because the efficacy of iM-targeted therapies seems to be dependent on the ability of the small molecule to shift the equilibrium between the folded and unfolded iM *in vivo. The objective of this thesis is to determine the thermal stability and pH stability of the seven model iMs before and after drug*

binding. This entails measuring changes in the iM T_m's (that is, the temperature at which 50% of the iM is folded) as a result of drug binding, which was accomplished by using UV-visible spectroscopy on a Cary 100 UV-visible spectrometer. To study the pH stability of these iMs, we measured changes to the iM pKa's (that is, the pH at which 50% of the iM is folded) as a result of drug binding. This was accomplished using circular dichroism studies on an Olis DSM-20 spectropolarimeter. Drug-DNA interactions were confirmed and described quantitatively using fluorescence emission spectroscopy on an ISS K2 fluorometer. This is a creative method for studying small molecule interaction with iMs that allowed us to understand, in a best case scenario, what changes small molecule binding can have on overall iM stability.

II.b. Methodology

Materials

The model iMs used in this study were based on the simple, iM-forming oligonucleotide known as T1.[17] The T1 iM is a good model because it undergoes a simple two-state transition from folded to unfolded form.[17] The ssDNA sequence known as HP6 (5'-AGTTTTAAA-3'), which is a known high-affinity target of 7-AAMD, was incorporated into each of T1's loop regions (**Fig. 4**), creating a total of seven model iMs. These oligos were synthesized by and purchased from Midland Certified Reagent Co., Inc. (Midland, TX). Each of the model iM oligonucleotide stock solutions were stored in a 10 mM Tris, 1 mM EDTA buffer at pH 8.0 in a -20℃ freezer. The sodium cacodylate, Tris-HCl, and EDTA used to create buffer solutions were purchased from Fisher Scientific (Pittsburgh, PA). 7-AAMD was also purchased from Fisher Scientific (Pittsburgh, PA) and stored in DMSO at -20℃. Technical note: it is important to aliquot the 7-AAMD solutions in DMSO into ~100 µL portions and store them at -20 °C. Repeated freezing

and thawing cycles rapidly degrades 7-AAMD fluorescence and DNA-binding properties via a mechanism that we are presently investigating.

K_d determination for 7-AAMD-iM interactions

Fluorescence titration studies were done using an ISS K2 Fluorometer. A 0.6 μM solution of 7-AAMD was excited with 530 nm light and emission spectra were collected from 560-700 nm after incremental additions of 1 mM iM. Emission spectra were collected until changes in emission reached a plateau, indicating saturation of the 7-AAMD. Relative changes in fluorescence ($\Delta F/F_o$) at emission λ_{max} (~625 nm) for each of the samples were plotted against amount of ssDNA titrated, and through application of a Langmuir isotherm fitting equation, dissociation constants (K_d) were calculated, as has been previously described.[44-46] These experiments were carried out both at acidic pH of 5.4 where the iM was fully folded and at an alkaline pH of 8 where no iM would normally be formed without facilitation.

Thermal Stability and Denaturation of iMs

iM structures show a pronounced hypsochromic and hyperchromic shift in their UV-visible absorbance spectra upon heating that can be monitored at 260 nm to determine folded and unfolded states. Model iMs (5 μM) in 30 mM cacodylate buffer at pH 5.4 were melted with and without 7-AAMD. Melting of the model iMs was performed on a Cary 100 UV-Visible Spectrometer (Agilent Technologies, Santa Clara, CA). Prior to experimentation, each sample was heated to 80℃ for 5 minutes and then cooled to room temperature to ensure removal of unwanted DNA dimers. Thermal denaturation recordings were made by monitoring the absorbance at 260 nm while increasing the temperature from 25℃ to 85℃, at a ramping rate of 2℃ per minute and a one-minute hold at each temperature. Calculated T_m's represent the temperature at which 50% of the model iM is unfolded. All thermal denaturation experiments could be fit to a simple two-state

model, defined in *Eq. 1)* as:

$$Eq.1)\ Unfolded \leftrightarrow Native$$

By applying this model, the absorbance data can allow estimation of the equilibrium constant, *K*, at any given temperature. The change in free energy at 37 °C ($\Delta G°_{37\ °C}$) can be calculated by the use of the absorbance data at 37℃ and *Eq. 2*:

$$Eq.2)\ K = \frac{[N]}{[U]} = e^{-\Delta G/RT}$$

where [N] and [U] are the concentrations of the iM and random coil forms of DNA, respectively, *R* is the gas constant, and *T* is the physiological temperature (310 K).

Determination of iM pK_a

To determine the pK_a for iM folding (defined as the pH at which 50% of the oligo is folded into the iM), CD spectra of DNA solutions at 20°C were collected from 250-320 nm at various pH's (pH 5 - pH 8) on an Olis DSM 20 Circular Dichroism (CD) instrument fitted with a peltier heat block (Olis, Inc. Bogart, GA, USA). The experiments were performed with and without 7-AAMD. An integration time as a function of high voltage was used. The CD signals observed at 290 nm were then plotted against pH, and *Eq. 3* was applied to obtain the pKa's of the model iMs and the cooperativity parameter that describes their unfolding.

$$Eq.3)\ Signal_{total} = \frac{signal_{folded} - signal_{unfolded}}{1 + 10^{cooperativity*(pH-pKa)}} + signal_{unfolded}$$

II.c Results

7-AAMD binds the model iMs

Binding of 7-AAMD to the model iMs results in significant changes to the fluorescence spectra of the drug, **(Fig. 5)** as has been described previously for binding of 7-AAMD to select ssDNA.[44-46] Analysis of these fluorescence changes allows for calculation of the binding affinity of the drug for each iM through application of a Langmuir isotherm fitting equation. The close resemblance of the spectral changes to 7-AAMD binding to ssDNA hairpins containing the HP6 sequence in their loops suggests that 7-AAMD is interacting with the loops of the model iMs.[44,46] The K_d's describing the interaction between 7-AAMD and the model iMs were determined and tabulated in **Table 1**.

The K_d's for L1HP, L2HP, and L3HP were 4-to-5 times lower at pH 5.4 than the K_d's determined at pH 8 **(Table 1)**. The fluorescence intensity change upon binding of the iMs by 7-AAMD is also lower at the more alkaline pH than the fluorescence intensities at the more acidic pH (**Fig .5**). These pH-dependent changes in the emission spectra are consistent with 7-AAMD's preference for the HP6 target in a hairpin conformation and the solvatochromic effects associated with binding of 7-AAMD to this particular ssDNA target.[46,48] Interestingly, this data also shows that is possible for a small molecule to preferentially bind the folded iM rather than the unfolded ssDNA, an ideal feature of future potential therapeutics that target the iM.

The number of assumed binding sites for each sequence influenced the calculated dissociation constants. At both pH 5.4 and 8.0, 7-AAMD was more readily bound by an iM with multiple binding sites than an iM with one binding site, with the exception of L13HP and L123HP at an acidic pH. We attribute this to sterics; when folded into the iM, the hairpin loops in the first and third position are directly adjacent to one another and can impede simultaneous ligand binding. As the iM unfolds at a higher pH, the DNA becomes linear. The potential binding sites for 7-AAMD become further apart and largely independent of one another, and as a result, the K_d for L13HP at pH 8 is less than L1HP or L3HP at pH 8.

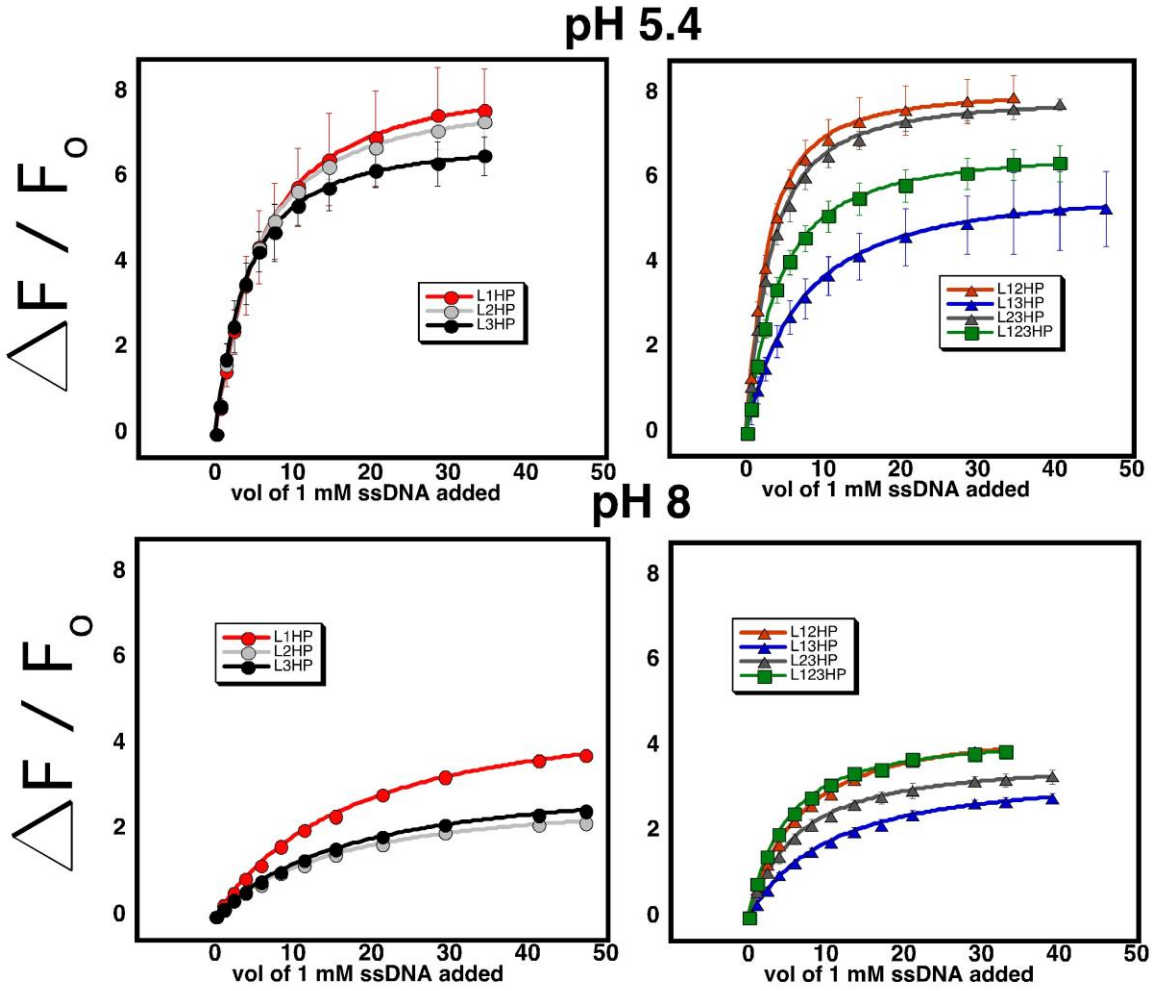

Figure 5. Titration curves derived from fluorescence intensification of 7-AAMD in the presence of the model iMs. Model iMs containing one hairpin loop are shown on the left. Model iMs containing multiple hairpin loops are shown on the right. The fluorescence intensifications and calculated dissociation constants are correlated (a phenomenon previously observed in earlier studies of 7-AAMD binding ssDNA[44-48]) and these two parameters are dependent on the pH of the solution.

Regardless of the small differences in 7-AAMD's affinity for our model iMs at an acidic pH, this data illustrates that 7-AAMD bound our model iMs. We interpreted this to mean that 7-AAMD's interaction with these iMs constitutes a useful model with which to probe the effects of small molecule binding to the iM. The following experiments explored those effects on the thermal and pH stability of the model iMs.

Table 1.) Dissociation constants describing the interaction of model iMs and 7-AAMD at acidic and alkaline pH's

	K_d (μM)	
	pH 5.4	pH 8
L1HP	2.70 ± 0.32	8.98 ± 1.15
L2HP	2.31 ± 0.13	8.18 ± 1.18
L3HP	1.73 ± 0.48	9.50 ± 0.93
L12HP	1.03 ± 0.05	3.01 ± 0.18
L13HP	3.18 ± 0.28	4.70 ± 0.51
L23HP	1.23 ± 0.17	2.98 ± 0.30
L123HP	1.72 ± 0.26	2.16 ± 0.17

7-AAMD affects the thermal stability of the model iMs

Previous reports have demonstrated that iM loop length, position, and composition affect both the thermal and pH-dependent stability of iMs.[9,50-52] Our lab has previously shown that iMs with loops in the second position are more stable than iMs with identical loops in the terminal first or third positions.[17] While those previous studies used loops exclusively composed of dT residues, here our model iMs contained more heterogeneous loop sequences. Specifically, the iMs used here contain the loop insert known as HP6.[46] HP6 alone binds 7-AAMD with a K_d of 0.4 μM but only minorly affects fluorescence intensity. We inserted the HP6 sequence into the first, second, and third loops of the model iMs, and all combinations. Similar to our lab's previous findings, iMs with loops in the first and third position have significantly lower T_m's than when the insert was at the second position. Interestingly, when compared to previously published data describing iMs

with poly-dT loops of equal length, the model iMs in this study have higher T_m's; for example, L1HP has a T_m ~10 °C higher than Mod1T10, an iM with a 10 bp poly-dT loop in the same position.[17] This is presumably due to the presence of intra-loop interactions. Future, more systematic studies will be needed to fully understand the effects of these intra-loop forces on iM thermal stability.

Model iMs with multiple hairpin loops exhibit interesting patterns in thermal stability. We anticipated that the HP6 loops would confer additional stability to the iM, given their ability to form an additional dA•dG base pair. However, our data shows that the presence of loops at any position negatively influences iM stability. Sequences with multiple hairpin loops like L12HP have a destabilizing "weighted average" effect, where the T_m of an iM containing multiple hairpin loops is between the T_m's of iMs that contain only one of the hairpins. This pattern is depicted graphically

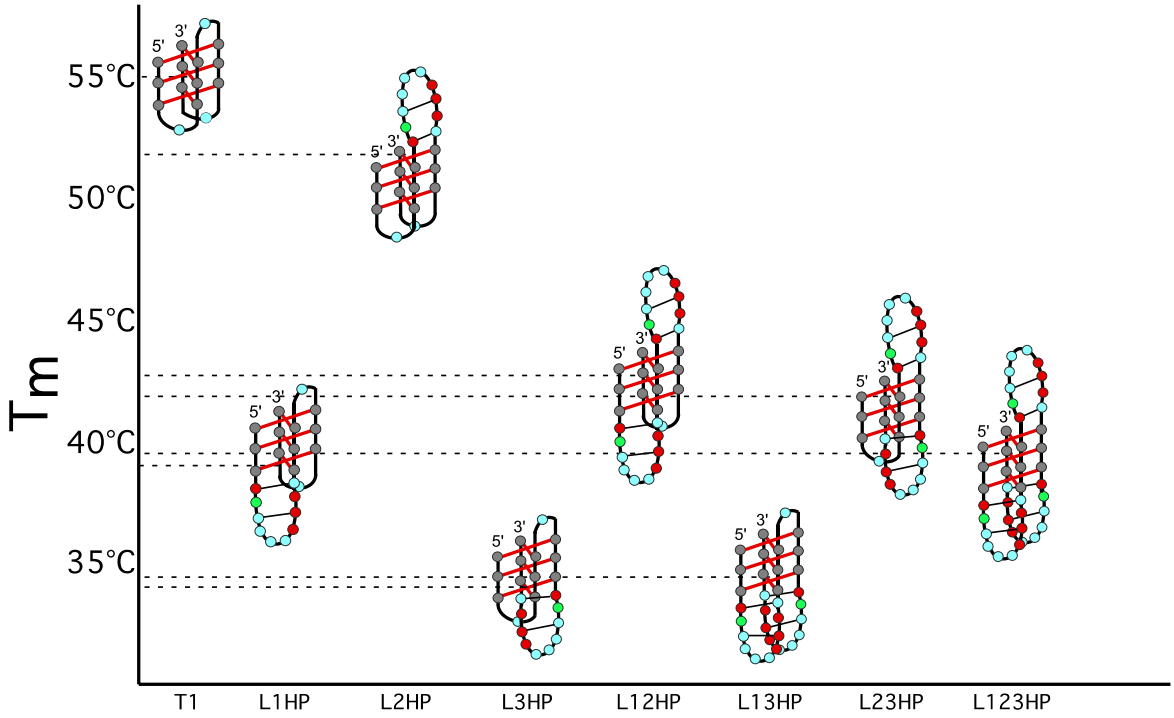

Figure 6. Graphical depiction of the "weighted average" destabilization effect describing the thermal stability of iMs containing multiple hairpin loops. Cytosines, adenines, thymines, and guanines are shown in grey, red, blue, and green, respectively. Note how the T_m for an iM with multiple loops falls between the T_m's of simpler iMs containing one of the loops. Also, note that regardless of hairpin loop placement, all model iMs are less thermally stable than the simple T1 iM.

Table 2. Calculated T_m's and $\Delta G°_{37}$ of the model iMs before and after saturation with 7-AAMD

	T_m (°C)		ΔT_m (°C)	$\Delta G°_{37°C}$ (kcal/mol)		$\Delta\Delta G°_{37°C}$ (kcal/mol)
	No 7-AAMD	7-AAMD		No 7-AAMD	7-AAMD	
L1HP	39.0 ± 1.4	39.6 ± 0.2	0.6	-1.8	-1.7	0.1
L2HP	51.8 ± 1.1	53.1 ± 0.4	1.3	-5.1	-5.4	-0.3
L3HP	34.0 ± 0.1	38.4 ± 0.5	4.4	0.8	-0.6	-1.4
L12HP	42.7 ± 0.4	47.1 ± 0.3	4.4	-2.4	-3.8	-1.4
L13HP	34.4 ± 1.8	36.4 ± 0.2	2.0	1.7	0.1	-1.6
L23HP	41.8 ± 0.3	45.7 ± 0.3	3.9	-2.3	-3.2	-0.9
L123HP	39.5 ± 0.1	35.6 ± 0.9	-3.9	-1.4	-0.3	1.1

in **Fig. 6** and tabulated in **Table 2.**

The T_m's for all model iM sequences with multiple hairpin loops followed this pattern, with the slight exception of L13HP. L13HP deviated negatively from the "weighted average" trend, with slightly lower than expected T_m's and pK_a's. We suspect this destabilization is due to steric interactions between the first and third hairpin loops that are present when L13HP is folded into the iM. It is unclear whether the "weighted average" effect is present in other iMs containing multiple loops, or if this phenomenon is unique to our model iMs. Still, the strategic incorporation of multiple loops into the iM may benefit nanotechnologists seeking to fine-tune the stability of iMs used in a litany of nanoscale processes, as described in several reviews.[53-55]

Past data has shown that 7-AAMD can affect the thermal stability of ssDNA structures. In fact, a past report revealed that 7-AAMD had the ability to shift the T_m of ssDNA hairpins containing the HP6 insert, in some cases by more than 30 °C.[46] Our fluorescence data indicated that 7-AAMD bound our model iMs very similarly to those ssDNA hairpins; logically, we anticipated stabilization of our model iMs.

The results were less dramatic than anticipated but notable. L1HP, L2HP, L13HP experienced little to no increase in T_m after binding of 7-AAMD. L3HP, L12HP, and L23HP experienced a modest T_m increase of ~4 °C after binding of 7-AAMD. Interestingly, binding of 7-AAMD to L123HP caused a decrease in T_m, lowering L123HP's T_m from 39.5 °C (above

physiological temperature) to 35.6 °C (below physiological temperature). After binding of 7-AAMD, L3HP's T_m was raised from 34.0 °C (below physiological temperature) to 38.4 °C (above physiological temperature). While the absolute change in T_m for these two models may be small, they could represent a therapeutically useful repositioning of equilibrium away from or towards formation of an iM *in vivo*. Changes in the absorbance data for the model iMs at 37 °C reveal that small molecule binding can affect the energetics of iM folding. The measured $\Delta\Delta G°_{37°C}$ values tabulated in **Table 2** are similar to those reported elsewhere that describe the effect of molecular crowding reagents on iM formation.[17,56]

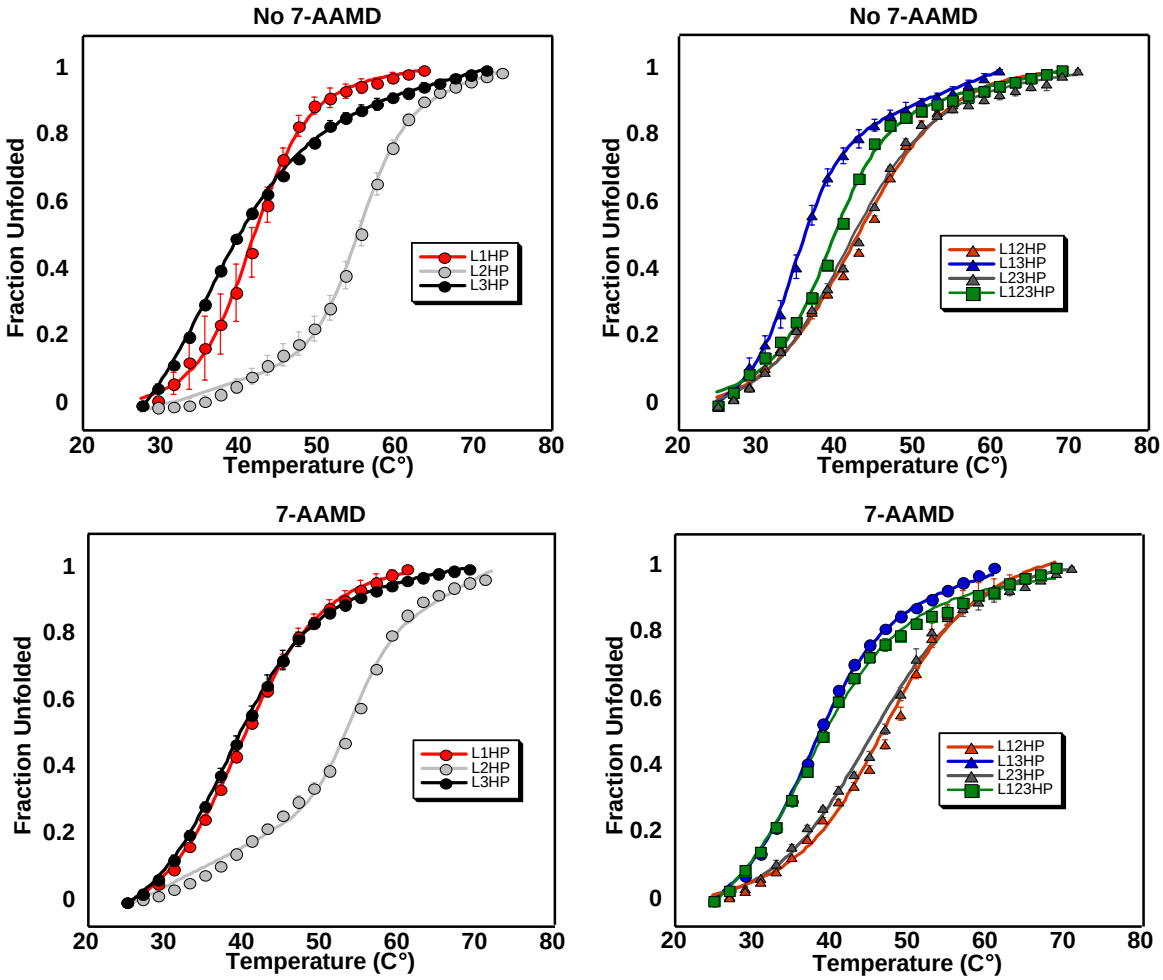

Figure 7. Thermally induced unfolding of the model iMs before and after saturation with 7-AAMD, as measured by hyperchromic shifts in absorbance upon heating. Model iMs containing one hairpin loop are shown on the left. Model iMs containing multiple hairpin loops are shown on the right. T_m's are tabulated in Table 2.

7-AAMD affects the pH dependency of the model iMs

Previous reports have similarly demonstrated that iMs with loops in the second position have higher pK_a values than iMs with loops in the first and third position.[17, 50-52] The pK_a values measured for L1HP, L2HP, and L3HP follow this trend as well. These models have slightly different pK_a values compared to iMs with poly-dT loops.[17] L1HP (pK_a 6.24) is slightly more stable than Mod1T10 (pK_a 6.14) and L2HP (pK_a 6.80) is slightly more stable than Mod2T10 (pK_a 6.62). However, L3HP (pK_a 5.96) was slightly less stable than Mod3T10 (pK_a 6.12). The pK_a values for model iMs with multiple hairpin loops followed the same "weighted average trend" that described their relative thermal stabilities, where the pK_a for L12HP falls between the pK_a values of L1HP and L2HP.

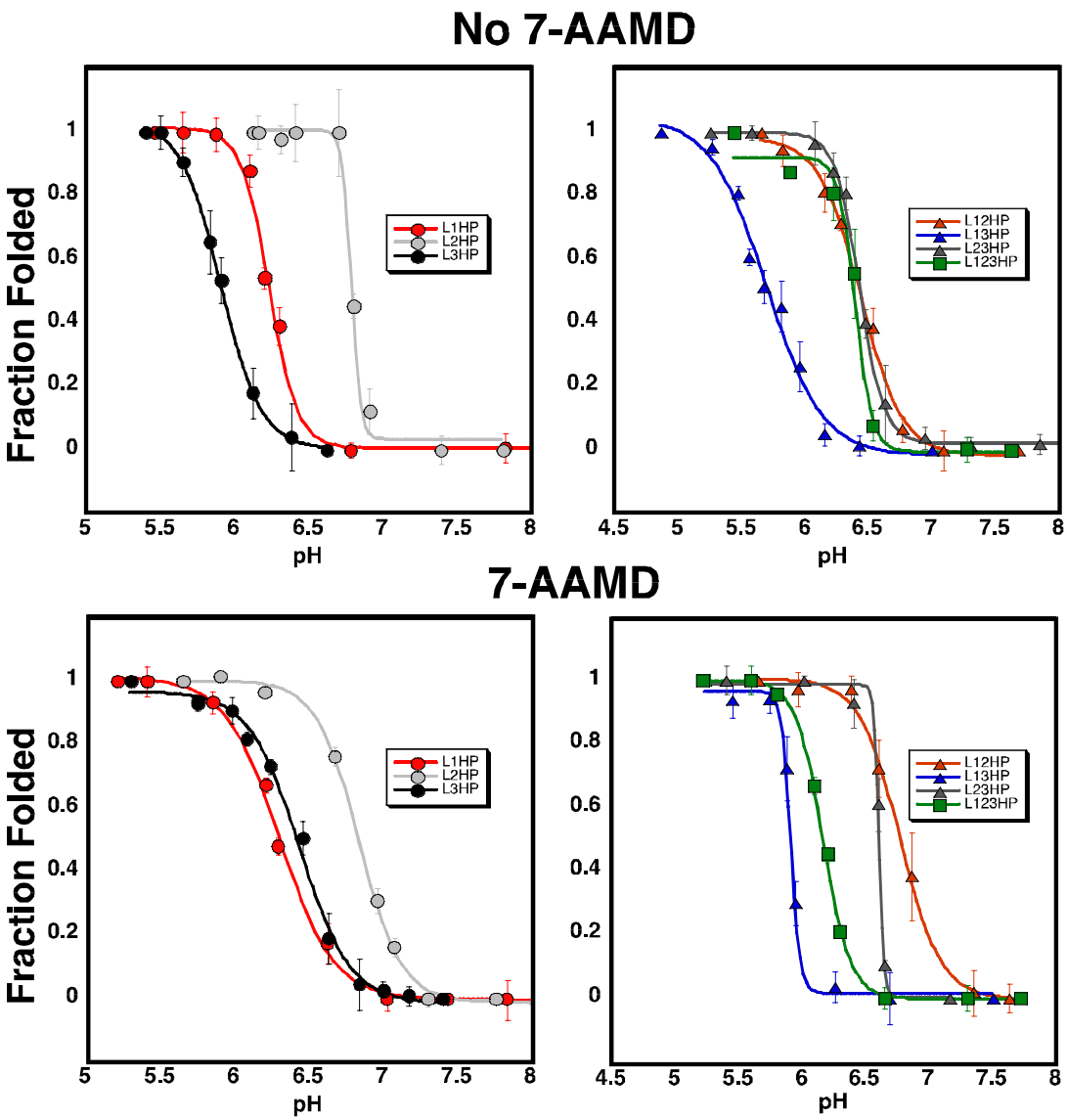

Figure 8. pH-induced unfolding of the model iMs before and after saturation with 7-AAMD, as monitored by CD signal at 290 nm. Model iMs containing one hairpin loop are shown on the left. Model iMs containing multiple hairpin loops are shown on the right. Calculated pK_a's are tabulated in Table 3.

The modest effects of 7-AAMD binding on the thermal stability of the model iMs were reflected in the pK_a studies. L1HP and L2HP experienced pK_a increases of ~0.1 pH units. L13HP and L23HP experienced pK_a increases of ~0.2 pH units, and L12HP experienced a pK_a increase of ~0.3 pH units. L123HP's modest thermal destabilization after ligand binding was accompanied by a modest decrease in pK_a of ~0.2 pH points, further supporting the notion that simultaneous interaction with all loops may be a viable method for destabilizing the iM *in vivo*.

Surprisingly, L3HP experienced an increase in pK_a of nearly 0.5 pH points after binding of 7-AAMD. As mentioned above, the L3HP model iM also experienced a modest T_m increase of ~4°C after ligand binding. Prior to ligand binding, L3HP was one of the least stable model iMs; it had the lowest T_m (34.0 °C) and the second lowest pK_a (5.96). This result suggests that, if the goal of iM-targeted therapies is to dramatically shift the iM's stability, semi-stable iMs, perhaps with unique loops in the third position, may be appealing targets.

Table 3. Calculated pKa's for model iMs before and after saturation with 7-AAMD

	pK_a						
	L1HP	L2HP	L3HP	L12HP	L13HP	L23HP	L123HP
No 7-AAMD	6.24 ± 0.01	6.80 ± 0.01	5.96 ± 0.05	6.46 ± 0.02	5.70 ± 0.01	6.43 ± 0.01	6.40 ± 0.02
7-AAMD	6.32 ± 0.01	6.90 ± 0.01	6.45 ± 0.01	6.79 ± 0.11	5.92 ± 0.01	6.61 ± 0.01	6.18 ± 0.01
ΔpK_a	0.08	0.10	0.49	0.33	0.22	0.18	-0.22

II.d Discussion

Our primary goal for this thesis was to create a series of model iMs that could facilitate small molecule interaction with loop regions of the DNA iM and to subsequently measure changes in iM stability. To create these model iMs, we inserted a short hairpin sequence of ssDNA into each of the loop regions of a simple iM. We chose this sequence because of its conformation-dependent affinity for the antitumor drug 7-AAMD. To determine if 7-AAMD interacted with the model iMs, we monitored the unique fluorescent properties of the molecule to confirm interaction with the iMs. We then measured the T_m's, $\Delta G°_{37\,°C}$'s, and pK_a's of the model iMs before and after saturation with 7-AAMD to determine the effects of small molecule binding on iM stability.

This data is important because it allows researchers to better understand the extent to which loop-binding small molecules can affect the folding of iMs. This directly impacts the feasibility of iMs as drug targets for gene therapy. While our findings were less dramatic than anticipated, they illustrate that by simultaneous changes to iM T_m, pK_a, and $\Delta G°_{37\,°C}$, small molecule binding can

be another important energetic consideration that affects the formation of iMs *in vivo*, especially for semi-stable iMs with T_m's and pK_a's near physiological values. However, our findings also suggest that *dramatically* shifting the stability of the iM *in vivo* via loop-binding small molecules may be a difficult task for future gene targeting applications. Until more iM-interactive compounds can be identified that dramatically alter the stability of iMs, our experiments suggest that the future of iM-targeting may be better suited for combination therapies as described by Hurley rather than standalone therapies.[34] Additionally, our experiments make no conclusions about the ability of proteins or thoughtfully designed peptidomimetic ligands to affect iM stability, two very promising strategies illustrated by other groups.[33,57] Our results suggest that, if the goal of iM targeting is to dramatically alter iM stability, identification or synthesis of iM-interactive proteins and biomimetics may be a worthwhile pursuit.

II.e Summary

The iM was originally dismissed as a biophysical novelty with no real biological significance, but through the contributions of researchers across many disciplines, we have come to understand the iM as 1.) a dynamic ssDNA structure that cells use to modulate expression of genes critical to their survival, and 2.) a very appealing drug target for gene therapies, specifically those seeking to provide anti-cancer benefit. Today, many "targeted" contemporary cancer treatments are "anti-protein" in that they seek to inhibit a particular oncogenic protein. iM and G4 targeted therapies are unique in that they are "anti-gene" treatments; they are able to directly inhibit the transcription of overactive oncogenes. These types of therapies would be of great use in the field of oncology. However, the development of these therapies necessitates a deeper understanding of the effect small, drug-like molecules can have on overall iM stability, as

this directly influences the efficacy of therapies targeting the iM. This thesis concluded that a small, loop-binding molecule can in fact modestly affect iM stability. However, it would also seem that future therapies seeking to *dramatically* affect iM stability *in vivo* via small molecules will be a difficult (but not impossible) endeavor.

II.f Future Work

This work has sought to explore the role small molecule binding can have on iM stability, but these experiments were performed in dilute aqueous buffer. Crowded solvent systems more closely mimic the intranuclear environment in which iMs actually form, and past studies have shown that iMs are almost always stabilized in these solvent systems. As a result, we are attempting to study the effects of small molecule binding to our model iMs in crowded solvent systems that more closely represent their native, intranuclear environment. However, solvaotchromic changes in the fluorescent properties of 7-AAMD have necessitated the use of different spectroscopic techniques to confirm and monitor DNA-drug interactions, namely UV-visible absorbance and fluorescence anisotropy.

REFERENCES

LIST OF REFERENCES

1. Watson, J.D., Crick, Francis. “Molecular structure of nucleic acid.” *Nature*, 171.737 (1953): 737-738.

2. Nelson, David L., L. Lehninger, Albert, Cox, Michael M. *Lehninger principles of biochemistry*. Macmillan, 2008.

3. Wells, R.D., et al., “The chemistry and biology of unusual DNA structures adopted by oligopurine oligopyrimidine sequences.” *The FASEB Journal*, 2.14 (1988): 2939-2949.

4. Bochman, Matthew L., Katrin Paeschke, Virginia A. Zakian. "DNA secondary structures: stability and function of G-quadruplex structures." *Nature Reviews. Genetics*, 13.11. (2012): 770.

5. Biffi, Giulia, et al. "Quantitative visualization of DNA G-quadruplex structures in human cells." *Nature Chemistry*, 5.3 (2013): 182-186.

6. Sun, D., L.H. Hurley. “The importance of negative superhelicity in inducing the formation of G-quadruplex and i-motif structures in the c-Myc promoter: implications for drug targeting and control of gene expression.” *Journal of Medicinal Chemistry*. 52(9) (2009): 2863-2874.

7. Rodriguez, R., et al., “Small molecule-induced DNA damage identifies alternative DNA structures in human genes.” *Nature Chemical Biology*. 8(3) (2012).

8. Huppert, J.L., Balasubramanian, S. “G-quadruplexes in promoters throughout the human genome.” *Nucleic Acids Research.* 35(2) (2007): 406-413.

9. Brooks, T.A., Kendrick, S., Hurley, L. H. “Making sense of G-quadruplex and i-motif

functions in oncogene promoters." *The FEBS Journal*. 277(17) (2010): 3459-3469.

10. Langridge, R., A. Rich. "Molecular structure of helical polycytidylic acid." *Nature*. 198(4882) (1963): 725-728.

11. Gehring, K., J.-L. Leroy, and M. Guéron. "A tetrameric DNA structure with protonated cytosine-cytosine base pairs." *Nature* 363(6429) (1993): 561.

12. Bhavsar-Jog, Y.P., et al., "Epigenetic modification, dehydration, and molecular crowding effects on the thermodynamics of i-motif structure formation from C-rich DNA." *Biochemistry,* 53(10) (2014): 1586-1594.

13. Olsen, C.M., W.H. Gmeiner, and L.A. Marky. "Unfolding of G-Quadruplexes: Energetic, and Ion and Water Contributions of G-Quartet Stacking." *The Journal of Physical Chemistry B,* 110(13) (2006): 6962-6969.

14. Miyoshi, D., A. Nakao, and N. Sugimoto. "Molecular Crowding Regulates the Structural Switch of the DNA G-Quadruplex." *Biochemistry,* 41(50) (2002): 15017-15024.

15. Cui, J., Waltman, P., Le, V. H., Lewis, E. A. "The effect of molecular crowding on the stability of human c-MYC promoter sequence i-motif at neutral pH." *Molecules,* 13 (2013): 127541-12767

16. Rajendran, A., Nakano, S., Sugimoto, N. "Molecular crowding of the cosolutes induces an intramolecular i-motif structure of triplet repeat DNA oligomers at neutral pH." *Chemical Communications,* 46 (2010): 1299-1301

17. Reilly, S.M., et al., "Effect of Interior Loop Length on the Thermal Stability and pKa of i-Motif DNA." *Biochemistry,* 54(6) (2015): 1364-1370.

18. Zeraati, M., et al., "I-motif DNA structures are formed in the nuclei of human cells." *Nature Chemistry,* 10(6) (2018): 631.

19. Hurley, L.H., et al., “G-quadruplexes as targets for drug design.” *Pharmacology & Therapeutics,* 85(3) (2000): 141-158.

20. Brooks, T.A., Hurley, L. H. “Targeting MYC expression through G-quadruplexes.” *Genes & Cancer,* 1(6) (2010): 641-649.

21. Guo, K., et al., “Formation of Pseudosymmetrical G-Quadruplex and i-Motif Structures in the Proximal Promoter Region of the RET Oncogene.” *Journal of the American Chemical Society,* 129(33) (2007): 10220-10228.

22. Xu, Y. and H. Sugiyama. “Formation of the G-quadruplex and i-motif structures in retinoblastoma susceptibility genes (Rb).” *Nucleic Acids Research,* 34(3) (2006): 949-954.

23. Kendrick, S., et al., “The i-motif in the bcl-2 P1 promoter forms an unexpectedly stable structure with a unique 8:5:7 loop folding pattern.” *Journal of the American Chemical Society,* 131(48) (2009): 17667-17676.

24. Dai, J., Hatzakis, E., Hurley, L. H., Yang, D. “I-motif structures formed in the human c-MYC promoter are highly dynamic−insights into sequence redundancy and I-motif stability.” *PloS One,* 1(5) (2010)

25. Bucek, P., R. Gargallo, and A. Kudrev. “Spectrometric study of the folding process of i-motif-forming DNA sequences upstream of the c-kit transcription initiation site.” *Analytica Chimica Acta,* 683(1) (2010): 69-77.

26. Sutherland, C., et al., “A Mechanosensor Mechanism Controls the G-Quadruplex/i-Motif Molecular Switch in the MYC Promoter NHE III1”. *Journal of the American Chemical Society,* 138(42) (2016)14138-14151.

27. Fedoroff, O.Y., et al., “Cationic Porphyrins Promote the Formation of i-Motif DNA and Bind Peripherally by a Nonintercalative Mechanism.” *Biochemistry,* 39(49) (2000): 15083-

15090.

28. Sedghi Masoud S., T.Y., Iida K., Nagasawa K., *Heterocycles*, 90 (2012)

29. Wang, L., et al., "The interactions of phenanthroline compounds with DNAs: Preferential binding to telomeric quadruplex over duplex." *International Journal of Biological Macromolecules*, 52 (2013):1-8.

30. Gao, N., Y. Wang, and C. Wei. "Interactions of phenanthroline compounds with i-motif DNA." *Chemical Research in Chinese Universities*, 30(3) (2014): 495-499.

31. Wright, E.P., et al., "Mitoxantrone and Analogues Bind and Stabilize i-Motif Forming DNA Sequences." *Scientific Reports*, 6 (2016): 394596.

32. Kendrick, S., et al., "The dynamic character of the BCL2 promoter i-motif provides a mechanism for modulation of gene expression by compounds that bind selectively to the alternative DNA hairpin structure." *Journal of the American Chemical Society*, 136(11) (2014): 4161-6171.

33. Kang, H.J., et al., "The transcriptional complex between the BCL2 i-motif and hnRNP LL is a molecular switch for control of gene expression that can be modulated by small molecules." *Journal of the American Chemical Society*, 136(11) (2014): 4172-4185.

34. Kendrick, S., et al., "Simultaneous Drug Targeting of the Promoter MYC G-Quadruplex and BCL2 i-Motif in Diffuse Large B-Cell Lymphoma Delays Tumor Growth." *Journal of Medicinal Chemistry*, 60(15) (2017): 6587-6597.

35. Sedghi Masoud, S. and K. Nagasawa. "i-Motif-Binding Ligands and Their Effects on the Structure and Biological Functions of i-Motif." *Chemical and Pharmaceutical Bulletin*, 66(12) (2018): 1091-1103

36. Kaiser, C.E., et al., "Insight into the Complexity of the i-Motif and G-Quadruplex DNA

Structures Formed in the KRAS Promoter and Subsequent Drug-Induced Gene Repression." *Journal of the American Chemical Society*, 139(25) (2017): 8522-8536.

37. Brown, R.V., et al., "The Consequences of Overlapping G-Quadruplexes and i-Motifs in the Platelet-Derived Growth Factor Receptor β Core Promoter Nuclease Hypersensitive Element Can Explain the Unexpected Effects of Mutations and Provide Opportunities for Selective Targeting of Both Structures by Small Molecules To Downregulate Gene Expression." *Journal of the American Chemical Society*, 139(22) (2017): 7456-7475.

38. Shu, B., et al., "Syntheses and evaluation of new acridone derivatives for selective binding of oncogene c-myc promoter i-motifs in gene transcriptional regulation." *Chemical Communications*, 54(16) (2018): 2036-2039.

39. Mueller, W.C., D.M. *Journal of Molecular Biology*, 35 (1968): 251-290.

40. Sentenac, A.S., E.J. Fromageot, P. *Biochimica et Biophysica Acta*, 161 (1968): 299-308.

41. Aivasashvilli, V.A.B., R. Sh. *FEBS Letters*, 160 (1983): 124-128.

42. Straney, D.C.C., D.M. *Biochemistry*, 26 (1987): 1987-1995.

43. White, R.J.P., D.R., *Biochemistry*, 27 (1988): 9122-9132.

44. Wadkins, R.M. and T.M. Jovin. "Actinomycin D and 7-aminoactinomycin D binding to single-stranded DNA." *Biochemistry*, 30(39) (1991): 9469-9478.

45. Wadkins, R.M., et al., "Actinomycin D Binding to Single-stranded DNA: Sequence Specificity and Hemi-intercalation Model from Fluorescence and1H NMR Spectroscopy." *Journal of Molecular Biology*, 262(1) (1996): 53-68.

46. Wadkins, R.M., B. Vladu, and C.-S. Tung. "Actinomycin D Binds to Metastable Hairpins in Single-Stranded DNA." *Biochemistry*, 37(34) (1998): 11915-11923.

47. Wadkins, R.M., et al., "The Role of the Loop in Binding of an Actinomycin D Analog to

Hairpins Formed by Single-Stranded DNA." *Archives of Biochemistry and Biophysics*, 384(1) (2000): 199-203.

48. Vekshin, N., et al., "Solvatochromism of the Excitation and Emission Spectra of 7-Aminoactinomycin D: Implications for Drug Recognition of DNA Secondary Structures." *The Journal of Physical Chemistry B,* 105(35) (2001): 8461-8467.

49. Molnar, M.M., S.C. Liddell, and R.M. Wadkins. "Effects of Polyamine Binding on the Stability of DNA i-Motif Structures." *ACS Omega*, 4(5) (2019): 8967-8973.

50. Benabou, S., et al., "Understanding the effect of the nature of the nucleobase in the loops on the stability of the i-motif structure." *Physical Chemistry Chemical Physics,* 18(11) (2016): 7997-8004.

51. Fujii, T. and N. Sugimoto. "Loop nucleotides impact the stability of intrastrand i-motif structures at neutral pH." *Physical Chemistry Chemical Physics*, 17(26) (2015): 16719-16722.

52. Fleming, A.M., et al., "Unraveling the 4 n− 1 rule for DNA i-motif stability: base pairs vs. loop lengths." *Organic & Biomolecular Chemistry,* 16(24) (2018): 4537-4546.

53. Alba, J.J., A. Sadurní, and R. Gargallo. "Nucleic acid i-motif structures in analytical chemistry." *Critical Reviews in Analytical Chemistry*, 46(5) (2016): 443-454.

54. Dembska, A., "The analytical and biomedical potential of cytosine-rich oligonucleotides: a review." *Analytica Chimica Acta,* 930 (2016): 1-12.

55. Yatsunyk, L.A., O. Mendoza, and J.-L. Mergny. ""Nano-oddities": unusual nucleic acid assemblies for DNA-based nanostructures and nanodevices." *Accounts of Chemical Research,* 47(6) (2014): 1836-1844.

56. Bhavsar-Jog, Y.P., et al., "Epigenetic Modification, Dehydration, and Molecular Crowding Effects on the Thermodynamics of i-Motif Structure Formation from C-Rich DNA."

Biochemistry, 53(10) (2014): 1586-1594.

57. Debnath, M., et al., "Preferential targeting of i-motifs and G-quadruplexes by small molecules." *Chemical Science*, 8(11) (2017): 7448-7456.

VITA

Lane Parmely grew up with a twin brother on a small farm in rural, unincorporated Pocahontas, Tennessee. Upon graduating from Middleton High School in 2013, he earned a full scholarship to Austin Peay State University in Clarksville, Tennessee. Originally a physics student, he felt more drawn to biochemistry, and he switched programs. He excelled in the Department of Chemistry, and his many faculty mentors there encouraged him to pursue summer research opportunities at other, larger universities. This led him to contact Dr. Randy Wadkins at the University of Mississippi, who welcomed him into his lab for two consecutive summers.

Upon graduating from Austin Peay State University in 2017 with a Bachelor's degree in Biochemistry, Lane returned to the University of Mississippi as a graduate student to continue his biophysical studies of noncanonical DNA structures. There, he enthusiastically served as a teaching assistant for general chemistry and biochemistry labs. After two years, he successfully defended his thesis, earning a Masters degree in Chemistry. Currently, Lane is attending medical school at Washington University in St. Louis on a full scholarship. As a researcher, he hopes to one day have a lab of his own, and as a physician, he hopes to reform the discrepancies in health care that marginalized populations experience today.

He is a first generation college student, and he is the first in his extended family to earn a graduate degree.